Effective carrier type and field dependence of the reduced-T_c superconducting state in $SrFe_{2-x}Ni_xAs_2$

N. P. Butch,* S. R. Saha, X. H. Zhang, K. Kirshenbaum, R. L. Greene, and J. Paglione
Center for Nanophysics and Advanced Materials, Department of Physics, University of Maryland, College Park, Maryland 20742, USA
(Received 15 November 2009; revised manuscript received 4 January 2010; published 27 January 2010)

Measurements of the Hall effect, thermoelectric power, magnetic susceptibility, and upper and lower critical fields were performed on single crystals of $SrFe_{2-x}Ni_xAs_2$, an FeAs-based superconducting system that exhibits a reduced superconducting transition temperature T_c in comparison to most other iron-pnictide superconductors. Studies of the Hall and thermoelectric responses indicate that Ni substitution in this system results in a dominant electronlike response, consistent with electron doping in other similar systems but with a weaker change in the Hall coefficient and a more gradual change in the thermoelectric response with Ni concentration. For optimally doped samples with full superconducting volume fraction, the lower and upper critical fields were determined to be $H_{c1}(1.8\ \mathrm{K})=0.08$ T and $H_{c2}(0)=25$ T, respectively, with lower-T_c samples showing reduced values and indications of inhomogeneous superconductivity. Comparable to other higher-T_c FeAs-based materials, the temperature dependence of the upper critical field, $\partial H_{c2}/\partial T$, is linear over a wide temperature range, and the large values of $H_{c2}(0)$ greatly exceed conventional estimates of paramagnetic and orbital limits.

DOI: 10.1103/PhysRevB.81.024518 PACS number(s): 74.70.Xa, 72.15.Jf, 74.25.F−, 74.25.Ha

I. INTRODUCTION

Chemical substitution in the iron-pnictide "122" compounds, which form in the tetragonal $ThCr_2Si_2$ crystal structure, has uncovered a large class of superconductors. The superconducting state in these compounds is a topic of great interest, as it appears to have unconventional pairing symmetry[1,2] and exists in proximity to magnetic order. Understanding superconductivity in the iron pnictides may also offer insight into the unusual superconducting states in other classes of materials, such as the high-T_c cuprates, heavy-fermion intermetallics, and organic charge-transfer salts.[3] Transition-metal substitution can effectively electron dope the antiferromagnetic parent compound, yielding superconductivity when Co, Ni, Ru, Rh, Pd, and Ir replace Fe.[4–7] In contrast, significantly higher transition temperatures of 35 K are achieved via hole doping on the alkaline-earth site, although these values are still lower than the 55 K superconducting transitions seen in the related "1111" materials.

Despite their lower values of superconducting transition temperature T_c relative to the 1111 materials, the 122 compounds can be prepared as large single crystals and are well suited for experimental study. One particularly interesting aspect of the superconductivity in 122 materials is the similarity of maximal T_c, 20–25 K, regardless of the transition-metal substituent. In fact, this trend is known to be broken only in the case of $SrFe_{2-x}Ni_xAs_2$ (Ref. 4) and $SrFe_{2-x}Pd_xAs_2$,[5] both exhibiting $T_c<10$ K.

The temperature-chemical concentration phase diagram of $SrFe_{2-x}Ni_xAs_2$ (Fig. 1) was recently studied.[4] As with other iron-pnictide superconductors, Ni substitution into $SrFe_2As_2$ initially suppresses the magnetostructural transition temperature T_0, which for $SrFe_2As_2$ occurs at about 200 K. The transition can be tracked to $x=0.15$, where $T_0\approx 40$ K, but it is not observed in $x=0.16$. Superconductivity is observed in the concentration range $0.10\leq x\leq 0.22$ with the highest values of superconducting transition temperature $T_c\approx 9$ K for $0.15\leq x\leq 0.18$. Bulk superconductivity is confirmed at $x=0.15$ by the presence of full diamagnetic screening and a small specific-heat anomaly at T_c, whose magnitude is consistent with those observed in other 122 materials with comparable T_c values.[8] The superconducting "dome" is asymmetric with rather sharp onset and more gradual offset of superconductivity as a function of x. At the edges of the dome, the width in T of the superconducting transitions increases, and the diamagnetic screening fraction is substantially decreased. These characteristics may be taken as signatures of inhomogeneous superconductivity appearing at the edges of the superconducting phase region, even though the Ni distribution appears chemically homogeneous throughout the entire substitutional range.

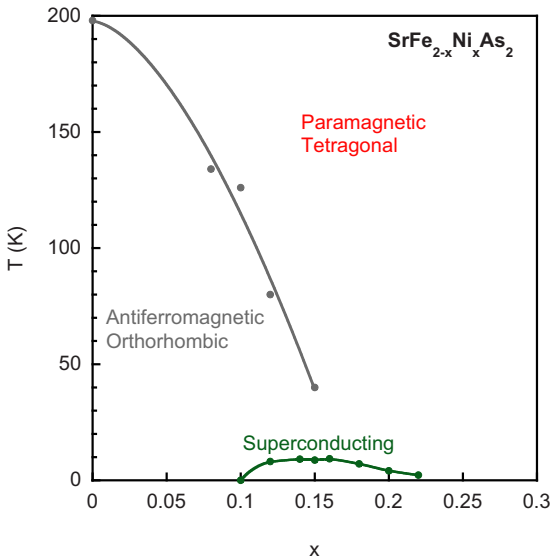

FIG. 1. (Color online) The phase diagram of $SrFe_{2-x}Ni_xAs_2$ as determined in Ref. 4. The magnetostructural transition is not observed for $x>0.15$ and superconductivity is found for $0.10\leq x\leq 0.22$. The maximum $T_c\approx 9$ K.

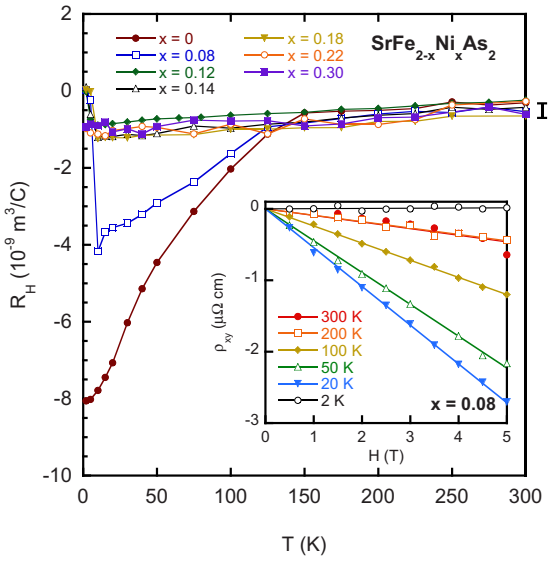

FIG. 2. (Color online) Hall coefficient of $SrFe_{2-x}Ni_xAs_2$ as a function of temperature. The magnetic transitions in $x=0$ and $x=0.08$ are evident as a drop in R_H. Superconducting transitions are evident for $0.08 \leq x \leq 0.22$ at low temperatures. All measurements are consistent with a dominant contribution from negative charge carriers. The error bar on the right illustrates the window of uncertainty of about $\pm 0.2 \times 10^{-9}$ m^3/C. Inset: field dependence of the transverse resistivity is linear to at least 5 T.

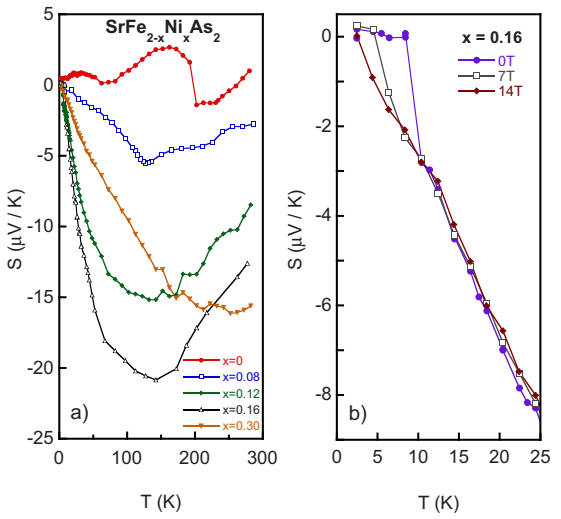

FIG. 3. (Color online) (a) Thermoelectric power S of $SrFe_{2-x}Ni_xAs_2$ vs temperature. The Ni-substituted samples exhibit linear T dependence at low temperatures, as would be expected in an electron-dominated metal. Slopes increase with increasing Ni content for $x<0.16$. (b) Magnetic field dependence of $S(T)$ illustrates the suppression of superconductivity for $x=0.16$.

In order to understand whether the reduced values of T_c in $SrFe_{2-x}Ni_xAs_2$ are entirely coincidental, or whether there is something fundamentally different about the superconductivity in this system, a study of the effective carrier type and the properties of the superconducting state was carried out on single crystals of $SrFe_{2-x}Ni_xAs_2$.

II. EXPERIMENTAL METHODS

Single crystals of $SrFe_{2-x}Ni_xAs_2$ were synthesized in excess FeAs and annealed in inert atmosphere. Details of sample preparation and characterization have been published.[4] Actual Ni concentration x was found to closely match nominal concentration. Measurements of the electrical resistivity, Hall effect, and thermoelectric power were carried out in a 14 T Quantum Design Physical Property Measurement System. Electrical resistivity was measured via a four-probe technique using low-frequency ac currents of 100 μA. Thermoelectric power was measured by applying a constant temperature difference of 0.7 K across each sample. Magnetization measurements were performed in a 7 T Quantum Design Magnetic Property Measurement System.

III. HALL EFFECT AND THERMOELECTRIC POWER

A comparison of the temperature T dependence of the Hall constant R_H for $SrFe_{2-x}Ni_xAs_2$ is shown in Fig. 2. The value of R_H was calculated from the slope of the symmetrized transverse electrical resistivity ρ_{xy} collected in magnetic fields $-5 \leq H \leq 5$ T. As shown in the inset of Fig. 2, the $\rho_{xy}(H)$ data are linear with a negative slope in $H<5$ T, indicating the existence of a dominant electronlike signal. For all Ni concentrations, these values of R_H at room temperature correspond to a density of carriers of about 10^{22} cm^{-3} in a one-band model. For $x=0$ and $x=0.08$, a change in carrier concentration coincides with the magnetostructural transition, yielding a low-T carrier concentration of 10^{21} cm^{-3}. For higher x, R_H is remarkably T independent, although the superconducting transition is readily discernable. A clear trend toward lower or higher carrier number with Ni substitution cannot be identified in these data. The uncertainty in the measurements is estimated at $\pm 0.2 \times 10^{-9}$ m^3/C, potentially masking any real x dependence in the data. In contrast, in the case of $BaFe_{2-x}Co_xAs_2$, such a trend is evident, with the variation in $R_H \geq 1 \times 10^{-9}$ m^3/C as a function of Co concentration.[9,10] While more precise Hall measurements are required to reach a conclusion about the actual variation in R_H for $SrFe_{2-x}Ni_xAs_2$, it seems clear that the magnitude is significantly smaller than that observed for the $BaFe_{2-x}Co_xAs_2$ system. For $SrFe_2As_2$, the low-T value of R_H determined in this study is slightly greater than half of a previously published value, -13×10^{-9} m^3/C,[11] and significantly less than -25×10^{-9} m^3/C found for $BaFe_2As_2$,[9,10,12] although the complex Fermi surface of these materials makes it difficult to make any direct comparisons of carrier density between Ba and Sr materials. These results are also consistent with angle-resolved photoemission spectroscopy results showing that there is a dominant electron Fermi surface in Co-substituted $BaFe_2As_2$.[13,14]

The temperature dependence of the thermopower S is shown in Fig. 3(a) for several values of x. The data qualitatively resemble those of $Ba(Fe_{1-x}Co_x)_2As_2$, which is superconducting, and $Ba(Fe_{1-x}Cu_x)_2As_2$, in which no trace of superconductivity has been found.[12] For the parent compounds $CaFe_2As_2$, $SrFe_2As_2$, and $BaFe_2As_2$, the magnetostructural

transition is evident in $S(T)$, and at lower temperatures, the T dependence is nonmonotonic. In $SrFe_2As_2$, $S(T)$ changes sign, which is also observed in $CaFe_2As_2$.[15] Upon electron doping, regardless of the alkaline-earth species, the thermopower is negative below room temperature. In $SrFe_{2-x}Ni_xAs_2$, the low-T thermopower data increase in magnitude monotonically, although a change in slope occurs at a higher x-dependent temperature. In the case of $x=0.08$, the local extremum in $S(T)$ corresponds to the magnetostructural transition. With increasing x, the extremum occurs at increasing T. However, at higher x it is not obviously correlated with any features in transport, magnetization, or heat capacity. While it is possible that the $S(T)$ minima might arise from changes in the Fermi surface, there are no corresponding features in the Hall data. An alternative explanation is that the relative mobilities of the various carrier species are changing. The magnitude of $S(T)$ is maximal with a value of about -20 μV/K at $x=0.16$, which has the highest superconducting transition temperature T_c. This value of S is less than half that of the maximum value in $Ba(Fe_{1-x}Co_x)_2As_2$ and is smaller also than that of $Ba(Fe_{1-x}Cu_x)_2As_2$. As in the Ba122 case, both $R_H(T)$ and $S(T)$ data sets are difficult to explain because there are multiple Fermi surfaces and the x dependence of magnetic interactions is complicated. However, the x-dependent change in $S(T)$ noted in the Ba compounds is not readily apparent in $SrFe_{2-x}Ni_xAs_2$, which features a more gradual change with x.

Figure 3(b) shows the magnetic field H dependence of $S(T)$ for $x=0.16$. Here, H was applied along the c axis. The superconducting transition is clearly visible, as its suppression by applied field, which is consistent with the electrical resistivity studies presented next.

IV. UPPER CRITICAL FIELD

The suppression with applied magnetic field H of the resistive superconducting transition of $SrFe_{2-x}Ni_xAs_2$ is illustrated in Fig. 4 for underdoped ($x=0.12$), optimally doped ($x=0.16$), and overdoped ($x=0.20$) concentrations. The data are normalized to the normal-state resistance for clarity. There is a clear qualitative change in the superconducting transitions across the superconducting concentrations. As noted previously,[4] the transition width is narrowest near optimal Ni concentrations. In fact, for $x=0.12$, the resistive transition is incomplete down to 1.8 K, as shown in Fig. 4, which may be due to macroscopic phase separation between superconductivity and antiferromagnetism, as is observed in $Ba_{1-x}K_xFe_2As_2$ by μSR measurements.[16] Note also that this is consistent with the zero-field $R(T)$ transition presented earlier,[4] in which a second step is clearly visible. This possibility is an interesting contrast to the case of $Ba(Fe_{1-x}Co_x)_2As_2$, which instead supports the microscopic coexistence of superconducting and magnetic order.[17,18] While local probes such as μSR or NMR are required for confirmation of true microscopic coexistence, these data suggest that electronic phase separation can arise also in the case of transition-metal substitution.

The superconducting upper critical field H_{c2}, with H applied parallel to the c axis, is shown in Fig. 5 for concentrations across the superconducting range. Here, H_{c2} is defined where the $R(T)$ data have half the normal-state value (0.5 in Fig. 4). With the exception of some curvature at low field, which is also seen in resistively determined values for other 122 superconductors,[19,20] the $H_{c2}(T)$ curves are strikingly linear. The slope $\frac{\partial H_{c2}}{\partial T}$ ranges from -1.8 T/K for $x=0.12$ to a maximum value of -2.9 T/K for $x=0.16$ at optimal doping, to -1.1 T/K for $x=0.22$. These slopes are comparable to those reported for $BaFe_2As_2$ and $SrFe_2As_2$ under pressure,[21] $EuFe_2As_2$ under pressure,[20] Co-substituted $SrFe_2As_2$ thin films,[22,23] $SrFe_{1.6}Co_{0.4}As_2$,[24] $Ba(Fe_{1-x}Co_x)_2As_2$,[19,25,26]

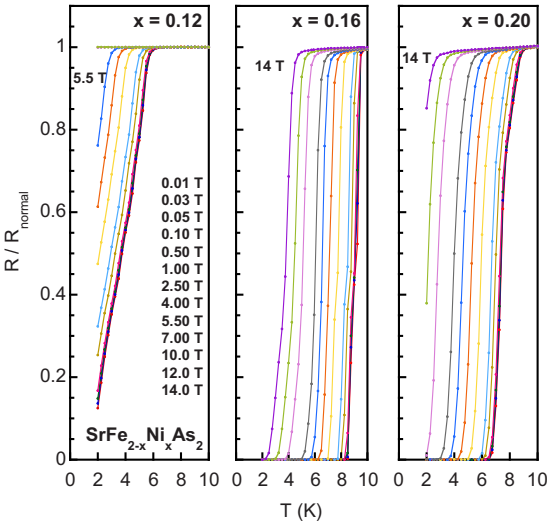

FIG. 4. (Color online) Electrical resistivity of $SrFe_{2-x}Ni_xAs_2$ vs temperature, showing the suppression of the superconducting transition by increasing magnetic field, applied parallel to the c axis. The resistivity is normalized to the normal-state value just above the transition. For $x=0.12$, 7 T data are not shown.

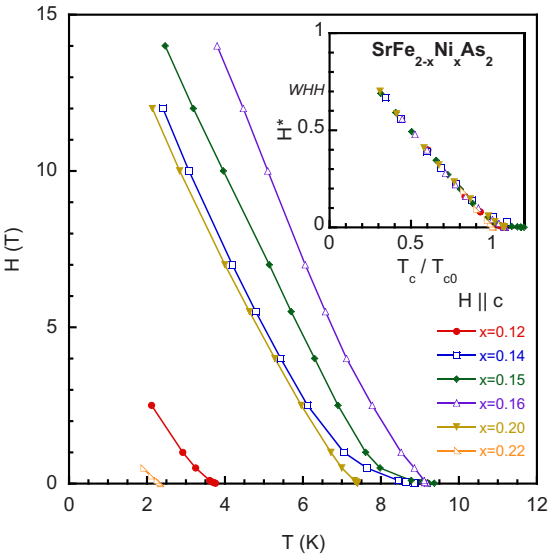

FIG. 5. (Color online) Upper critical field H_{c2} of $SrFe_{2-x}Ni_xAs_2$, for $H\|c$, vs temperature. The points here denote half of the resistive transition. Inset: H_{c2} curves scaled to the zero-field transition temperature T_{c0} and a slope of -1. The value of H_{c2} at $T=0$ K exceeds the WHH estimate.

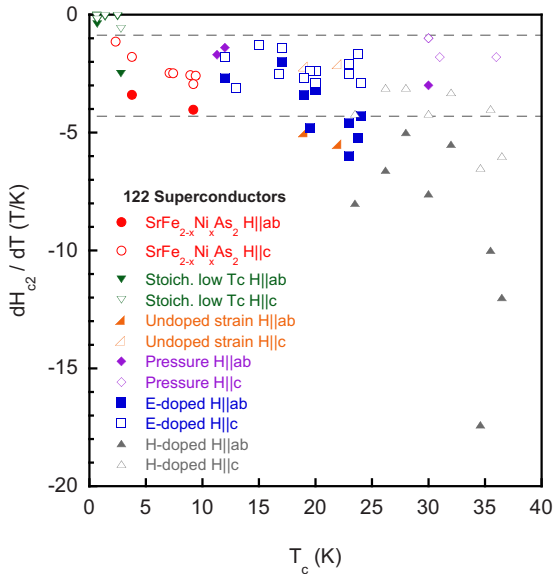

FIG. 6. (Color online) Upper critical field slope $\frac{\partial H_{c2}}{\partial T}$ of $SrFe_{2-x}Ni_xAs_2$ compared to values from the literature. Solid symbols denote H in plane while open symbols denote $H\|c$. For a large class of 122 superconductors, values of $\frac{\partial H_{c2}}{\partial T}$ are comparable despite a wide range of T_c values. Data for $SrFe_{2-x}Ni_xAs_2$ are from this work. Stoichiometric low-T_c materials include $SrNi_2P_2$ (Ref. 32), $SrNi_2As_2$ (Ref. 33), $BaNi_2As_2$ (Ref. 34), KFe_2As_2 (Ref. 35), $BaNi_2As_2$ (Ref. 36), and $BaNi_2P_2$ (Ref. 37). The other superconductors are discussed in the text. Data for "undoped strain" are from Refs. 30 and 31, "pressure" from Refs. 20, 21, and 38–40, "electron doped" from Refs. 19, 22–27, and 29 and "hole doped" from Refs. 41–48.

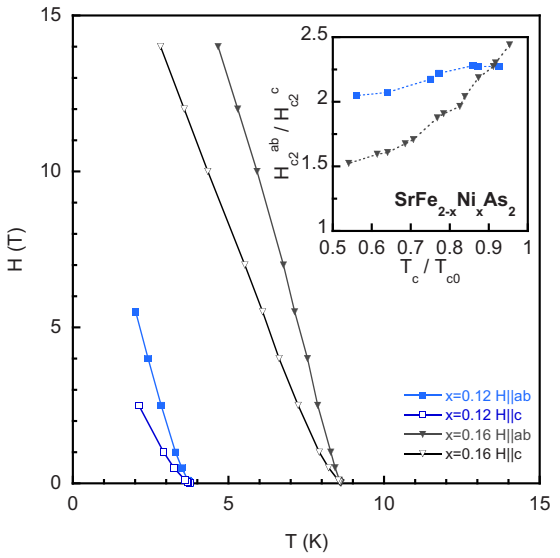

FIG. 7. (Color online) Upper critical field H_{c2} of $SrFe_{2-x}Ni_xAs_2$, determined via resistivity, for different field orientations. Inset: anisotropy of H_{c2}, which shows stronger temperature dependence at optimal doping.

$CaFe_{1.94}Co_{0.06}As_2$,[27] $BaFe_{1.91}Ni_{0.09}As_2$,[28] $CaFe_{1.94}Ni_{0.06}As_2$,[29] and ambient-pressure undoped strain-induced $SrFe_2As_2$ (Ref. 30) and $BaFe_2As_2$,[31] as illustrated in Fig. 6. This agreement is rather remarkable, given that these superconductors have values of T_c ranging from 20 K to more than 30 K, while the maximum value of T_c for $SrFe_{2-x}Ni_xAs_2$ is less than 10 K. Moreover, the response of the superconducting state to applied H seems insensitive to whether superconductivity has been stabilized by transition-metal substitution, applied pressure, or strain,[30,31] in the case of the undoped parent compounds. In contrast, hole-doped $SrFe_2As_2$ and $BaFe_2As_2$ feature larger values of $\frac{\partial H_{c2}}{\partial T}$.[41–48]

The inset of Fig. 5 shows the $H_{c2}(T)$ curves scaled with respect to T_{c0}, the value of T_c at $H=0$, and the reduced field $H^*=H_{c2}(-\frac{\partial H_{c2}}{\partial T}T_{c0})^{-1}$, which is defined such that the slope $\frac{\partial H^*}{\partial(T_c/T_{c0})}=-1$. As shown in the inset of Fig. 5, the scaling procedure collapses all $H_{c2}(T)$ data onto one curve, underscoring the already-noted similarity in H dependence for all superconducting concentrations of $SrFe_{2-x}Ni_xAs_2$. However, this plot also makes it clear that the Werthamer-Helfland-Hohenberg (WHH) estimate that $H_{c2}(0)\approx -0.7(T_{c0})\frac{\partial H_{c2}}{\partial T}$ is too low, because in $SrFe_{2-x}Ni_xAs_2$, $T_c/T_{c0}=0.3$ at $H^*=0.7$, where the WHH model predicts T_c should be 0.[49] At this low reduced temperature, the scaled upper critical curve is still linear, and shows no signs of saturation. In the presence of spin-orbit scattering and significant spin susceptibility, the value of $H_{c2}(0)$ would typically be suppressed with respect to the bare WHH estimate. In addition, the weak-coupling estimate of the paramagnetic critical field $H_P\approx 1.84T_c$ yields values comparable to those determined by the WHH formula. In other words, both conventional estimates of the paramagnetic and orbital-limiting fields underestimate the actual $H_{c2}(0)$. This characteristic has been noted in other iron-pnictide superconductors and is discussed in a recent review.[50]

An extrapolation of the linear $H_{c2}(T)$ slope to $T=0$ K yields a nominal limiting value of 25 T for $x=0.16$. Actually, this extrapolation may be quite accurate, as an almost linear $H_{c2}(T)$ is observed for $H\|c$ in Co-substituted $SrFe_2As_2$ thin films.[22] Superconducting coherence lengths $\xi=(\Phi_0/2\pi H_{c2})^{1/2}$, where Φ_0 is the flux quantum, range from about 10 to 3.5 nm for the range of $H_{c2}(0)$ values observed in $SrFe_{2-x}Ni_xAs_2$. For comparison, the value of $\xi=3$ nm was determined for $BaFe_{1.8}Co_{0.2}As_2$ via scanning tunneling microscopy.[51] Note that the low-H tails of the $H_{c2}(T)$ curves, which are rather large for $x=0.14$ and 0.15, have been ignored in the preceding analysis. Instead, the $H\rightarrow 0$ limiting slope has been fit above this region of large curvature because estimating $H_{c2}(0)$ using the low-H portion of the $H_{c2}(T)$ curves leads to an erroneous dramatic underestimate.

The $H_{c2}(T)$ curves were also studied with H applied perpendicular to the c axis. In Fig. 7, a field-direction comparison is made for $x=0.12$ and 0.16. As with all iron-based 122 superconductors, H applied perpendicular to the c axis suppresses T_c less quickly in $SrFe_{2-x}Ni_xAs_2$. Especially visible for $x=0.16$, there is increased curvature in $H_{c2}(T)$ relative to the $H\|c$ case, which is again consistent with measurements on Co-substituted $SrFe_2As_2$ thin films,[22] although due to the limited field and temperature range of the current measurements, it is unclear whether the $H_{c2}(T)$ curves extrapolate to the same value of H. The anisotropy H_{c2}^{ab}/H_{c2}^{c} is plotted in the inset of Fig. 7. The anisotropy in $x=0.12$ is roughly constant

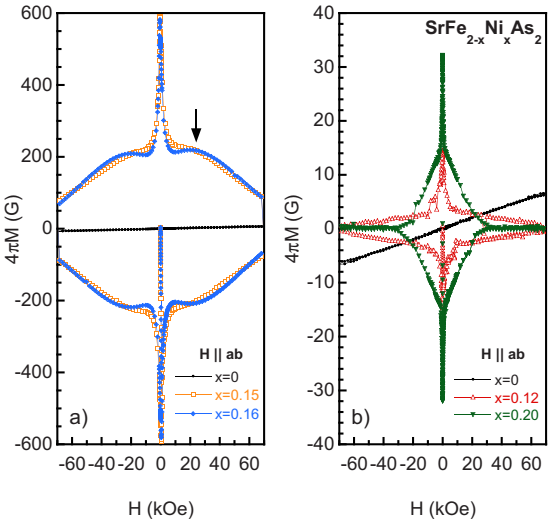

FIG. 8. (Color online) Magnetization of $SrFe_{2-x}Ni_xAs_2$ as a function of applied field at 1.8 K with H applied in plane. (a) Hysteresis loops for optimally doped samples have a large area and values of H_{c2} exceeding 7 T. The $x=0.16$ data exhibit a secondary peak, identified by the arrow. (b) For underdoped and overdoped samples, the loops are smaller and critical fields are lower. $M(H)$ data for the nonsuperconducting parent compound are shown for comparison. Note the different vertical scales. 10 kOe=1 T.

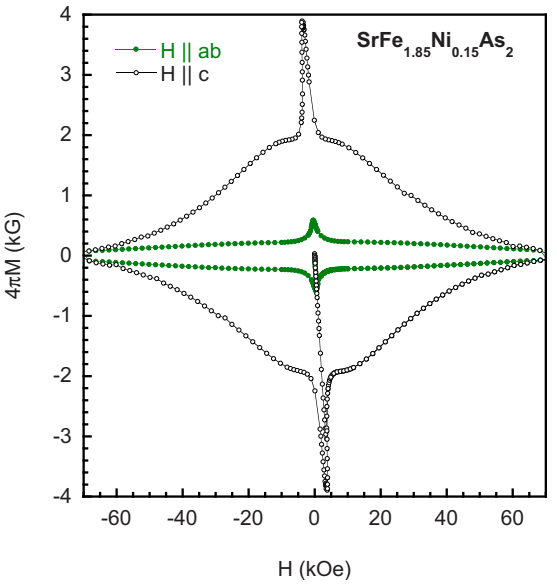

FIG. 9. (Color online) Direction dependence of the magnetization of $SrFe_{1.85}Ni_{0.15}As_2$ at 1.8 K. Field applied in plane evokes a much larger magnetic response than out of plane and the lower critical field H_{c1} is larger for $H\|c$. Demagnetization effects have been corrected for. 10 kOe=1 T.

at a value of about 2.2, whereas the anisotropy in $x=0.16$ varies from approximately 2.5 near T_c to 1.5 at $0.5T_c$. This range of anisotropy values is consistent with both electron-[19,25] and hole-doped 122 materials.[42,43,48] Considering the range of values of T_c exhibited by these superconductors, the similarity is again noteworthy.

V. MAGNETIC PROPERTIES

The field dependence of the superconducting state was also investigated via measurements of the magnetization $M(T,H)$. The low-H $M(T)$ data show that $SrFe_{2-x}Ni_xAs_2$ exhibits a full Meissner effect near optimal doping, for $0.14 \leq x \leq 0.16$.[4] In order to further compare the magnetic response of the superconducting state, the H dependence at 1.8 K was studied for x across the superconducting dome. As Fig. 8 shows, there is a clear difference between optimally doped samples, and the underdoped and overdoped samples. Note that the $x=0.12$ and $x=0.20$ data have had a normal-state contribution subtracted because the superconductivity does not fully occupy the bulk. Aside from expected differences in H_{c2} and the lower critical field H_{c1}, the area of the $M(H)$ loops is much larger near optimal doping. The $x=0.16$ sample exhibits a secondary peak, as has been observed in other electron-doped 122 compounds, although the local minima at low H can be much deeper in other systems.[28,58] In contrast, this phenomenon is not observed in the $x=0.15$ sample. Such fishtail structures in $M(H)$ hysteresis loops are thought to arise from vortex-pinning effects, which raises an interesting question about whether the appearance of this behavior for $x=0.16$ may be associated with the disappearance of magnetic order near $x=0.15$ (Fig. 1). However, a more systematic study is required to rule out simple disorder effects or sample dependence.

Turning to the $M(H)$ data for $x=0.12$, it is evident that the apparent value H_{c2} exceeds 7 T, as the $M(H)$ loop has nonzero area up to 7 T, whereas the superconducting transition appears to be already suppressed by this field in $\rho(T)$ data (Figs. 4 and 5). This effect may be the result of macroscopic phase separation between magnetic and superconducting regions in the sample, where there is no superconductive path between isolated superconducting sections. Alternatively, the nonzero area in $M(H)$ may be due to a small, uncorrected for ferromagnetic contribution, similar to that observed in undoped $SrFe_2As_2$.[30] In contrast, the $x=0.20$ sample exhibits the opposite: a much lower H_{c2} in $M(H)$ than in resistance data, which can be ascribed to the persistence of tiny connected regions of supercurrent that offer ineffective diamagnetic screening. In addition, the $M(H)$ data for $x=0.18$, which are not shown, exhibit inhomogeneous superconductivity, despite being chemically homogeneous as determined by energy-dispersive x-ray spectroscopy.[4] There exists a large variation in T_c and volume fraction between samples for $x \approx 0.12$ and $0.18 \leq x \leq 0.2$, suggesting that the superconducting region of the phase diagram is not really a rounded dome, but rather that the superconductivity onset and offset as a function of x are sharp. Again, local probes such as μSR or NMR are required to confirm this scenario.

It is instructive to check whether the anisotropy of the superconducting state evident from transport measurements is also seen in the $M(H)$ data. Figure 9 confirms that there is sizable magnetic anisotropy for optimally doped $x=0.15$. (Demagnetization effects have been corrected for.) With $H\|c$, the magnetization in the superconducting state is almost an order of magnitude larger than with H in plane. This behavior is consistent with that observed in

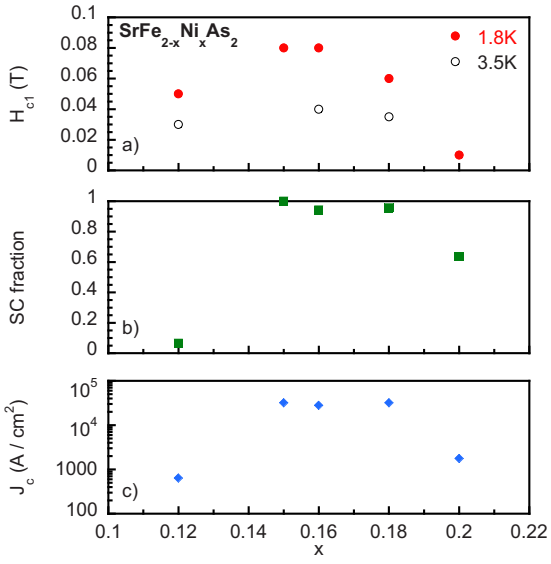

FIG. 10. (Color online) Concentration dependence of the low-temperature properties of the superconducting state of $SrFe_{2-x}Ni_xAs_2$. (a) The lower critical field H_{c1}, identified with the local minimum in the $M(H)$ virgin curve. (b) The superconducting volume fraction calculated from the initial slope of the virgin $M(H)$ curves at 1.8 K. (c) Superconducting critical current J_c, calculated using the Bean model.

$BaFe_{1.8}Co_{0.2}As_2$.[53] Concomitantly, the value of H_{c1}, as estimated from the local minimum in the virgin $M(H)$ curve, is larger for $H\|c$, with $H_{c1}^{c}=0.36$ T, than for $H\perp c$, with $H_{c1}^{ab}=0.08$ T. The initial slope of the virgin curve is consistent between the two H orientations and indicates full diamagnetic screening.

A summary of quantities derived from the low-T $M(H)$ data for $H\perp c$ is presented in Fig. 10. The values of H_{c1} were determined from the local minimum in the virgin $M(H)$ data. These values are about a factor of four larger than the value of H at which $M(H)$ starts to deviate from linearity. This alternative criterion for defining H_{c1} is more difficult to apply precisely because of curvature in $M(H)$ at fields below the local minimum. Estimates of the superconducting volume fraction are based on the initial slope of the virgin $M(H)$ curves and are consistent with values determined from low-H $M(T)$ data.[4] Magnitudes of the critical current J_c have been estimated using the Bean model. For the optimally doped samples, $J_c=3\times10^4$ A cm^{-2}, with $H\|ab$, while for $H\|c$, $J_c=2\times10^4$ A cm^{-2}. These values are about one order of magnitude lower than values quoted for $Ba(Fe,Co)_2As_2$,[25,26,28,52,53] $BaFe_{1.91}Ni_{0.09}As_2$,[28] and $BaFe_2(As_{0.68}P_{0.32})_2$.[54] The hole-doped 122 superconductors exhibit significantly higher values of $J_c\approx10^6$ A cm^{-2}.[42,44] Combining the values of H_{c1} and H_{c2}, it is possible to roughly estimate the magnitude of the penetration depth $\lambda=\frac{H_{c2}\xi}{\sqrt{2}H_c}$, where the thermodynamic critical field $H_c\approx(H_{c1}H_{c2})^{1/2}$. For both $x=0.12$ and $x=0.16$ with $H\|ab$, $\lambda^{ab}=50$ nm, while for $x=0.15$ with $H\|c$, $\lambda^{c}=20$ nm. In contrast, in $SrFe_{1.75}Co_{0.25}As_2$, values of $\lambda^{ab}=315$ nm and $\lambda^{c}=870$ nm were determined by μSR measurements.[55]

VI. DISCUSSION

The present study has uncovered several interesting properties of the $SrFe_{2-x}Ni_xAs_2$ system. First, neither the $R_H(T)$ or $S(T)$ data reflect an obvious increase in carriers, although both measurements appear to be dominated by negatively charged carriers. Second, despite the relatively lower values of T_c, there is nothing strikingly different about the superconducting state in $SrFe_{2-x}Ni_xAs_2$, at least in the bulk properties that have been probed in this study. However, it is intriguing that $\frac{\partial H_{c2}}{\partial T}$ values are comparable to those in electron-doped, pressure-induced, and strain-induced 122 superconductors, despite the variation in T_c (Fig. 6).

Recent angle-resolved photoemission measurements have revealed that in both K- and Co-substituted $BaFe_2As_2$, superconductivity requires the presence of both electron and hole pockets, and that the nesting conditions differ between hole- and electron-substituted materials.[13,56] This difference may explain the variation in T_c values, and perhaps even H_{c2} slopes, between the cases of hole and electron doping in the 122 materials. The multiband nature of the superconductivity can also explain the inapplicability of standard estimates of spin- and orbital-limiting critical fields.[50] It might further be expected that the disappearance of superconductivity would coincide with a change in Fermi surface. Indeed, it is argued that the temperature dependence of the Hall effect disappears at the end of the superconducting dome in $Ba(Fe_{1-x}Co_x)_2As_2$.[10] However, in the case of $SrFe_{2-x}Ni_xAs_2$, such an effect is not observed, as the values of R_H look to be independent of x to within experimental error. Moreover, there is no dramatic change in $S(T)$ as a function of x either, which suggests that variations in the Fermi surface between superconducting and normal states in $SrFe_{2-x}Ni_xAs_2$ are more subtle.

This absence of obvious changes in the Fermi surface is possibly related to the relatively narrow superconducting dome and the low values of T_c. The Fermi-surface topology required for superconductivity, e.g., for effective hopping in an $s_{\pm}$ model,[2] may be less well realized in $SrFe_{2-x}Ni_xAs_2$ compared to other 122 superconductors, over a smaller range of x, leading to a smaller number of superconducting carriers and lower T_c. This simple explanation does not, however, account for the similarity in $\frac{\partial H_{c2}}{\partial T}$ values. The apparent similarities between the superconducting states in different 122 materials must also be interpreted cautiously. For example, in both $SrFe_{2-x}Ni_xAs_2$ and pressure-induced 122 superconductors, full diamagnetic screening is observed over only part of the entire superconducting range.[21,57] However, this is not true for all electron-doped 122 compounds, because in $Ba(Fe_{1-x}Co_x)_2As_2$, full screening is observed for all superconducting concentrations.[58] Currently, it is not clear whether such differences are intrinsic or sample and measurement dependent. Experimental and theoretical investigation of the differences between the Fermi surfaces in Co- and Ni-substituted $SrFe_2As_2$ may help shed light on this issue.

To summarize, Hall effect and thermoelectric power measurements on $SrFe_{2-x}Ni_xAs_2$ are consistent with a dominant electronlike response, as is seen in other transition-metal substitution studies of 122 superconductors. The slope of the

upper critical field $\frac{\partial H_{c2}}{\partial T}$ is linear over a wide temperature range and appears to defy conventional estimates of paramagnetic and orbital limits. Despite lower values of T_c in this Ni-substitution series, values of $\frac{\partial H_{c2}}{\partial T}$ are comparable to other electron-doped 122 superconductors with higher T_c. For samples exhibiting maximum $T_c \approx 9$ K, full volume fraction superconductivity is observed, while samples exhibiting lower T_c seem to exhibit inhomogeneous superconductivity, with disconnected superconducting regions on the underdoped side and tiny connected regions of superconductivity on the overdoped side. Further investigation of possible magnetic/superconducting phase separation and details of the Fermi-surface evolution are called for.

ACKNOWLEDGMENTS

X.H.Z. and R.L.G. are supported by the NSF under Grant No. DMR-0653535. N.P.B. is supported by CNAM.

*nbutch@umd.edu

[1] D. Parker, M. G. Vavilov, A. V. Chubukov, and I. I. Mazin, Phys. Rev. B **80**, 100508(R) (2009).
[2] A. V. Chubukov, M. G. Vavilov, and A. B. Vorontsov, Phys. Rev. B **80**, 140515(R) (2009).
[3] N. P. Butch, M. C. de Andrade, and M. B. Maple, Am. J. Phys. **76**, 106 (2008).
[4] S. R. Saha, N. P. Butch, K. Kirshenbaum, and J. Paglione, Phys. Rev. B **79**, 224519 (2009).
[5] F. Han, X. Zhu, P. Cheng, G. Mu, Y. Jia, L. Fang, Y. Wang, H. Luo, B. Zeng, B. Shen, L. Shan, C. Ren, and H.-H. Wen, Phys. Rev. B **80**, 024506 (2009).
[6] W. Schnelle, A. Leithe-Jasper, R. Gumeniuk, U. Burkhardt, D. Kasinathan, and H. Rosner, Phys. Rev. B **79**, 214516 (2009).
[7] N. Ni, A. Thaler, A. Kracher, J. Q. Yan, S. L. Bud'ko, and P. C. Canfield, Phys. Rev. B **80**, 024511 (2009).
[8] S. L. Bud'ko, N. Ni, and P. C. Canfield, Phys. Rev. B **79**, 220516(R) (2009).
[9] F. Rullier-Albenque, D. Colson, A. Forget, and H. Alloul, Phys. Rev. Lett. **103**, 057001 (2009).
[10] L. Fang, H. Luo, P. Cheng, Z. Wang, Y. Jia, G. Mu, B. Shen, I. I. Mazin, L. Shan, C. Ren, and H.-H. Wen, Phys. Rev. B **80**, 140508(R) (2009).
[11] J.-Q. Yan, A. Kreyssig, S. Nandi, N. Ni, S. L. Bud'ko, A. Kracher, R. J. McQueeney, R. W. McCallum, T. A. Lograsso, A. I. Goldman, and P. C. Canfield, Phys. Rev. B **78**, 024516 (2008).
[12] E. D. Mun, S. L. Bud'ko, N. Ni, A. N. Thaler, and P. C. Canfield, Phys. Rev. B **80**, 054517 (2009).
[13] V. Brouet, M. Marsi, B. Mansart, A. Nicolaou, A. Taleb-Ibrahimi, P. Le Fèvre, F. Bertran, F. Rullier-Albenque, A. Forget, and D. Colson, Phys. Rev. B **80**, 165115 (2009).
[14] C. Liu, T. Kondo, R. M. Fernandes, A. D. Palczewski, E. D. Mun, N. Ni, A. N. Thaler, A. Bostwick, E. Rotenberg, J. Schmalian, S. L. Bud'ko, P. C. Canfield, and A. Kaminski, arXiv:0910.1799 (unpublished).
[15] M. Matusiak, Z. Bukowski, and J. Karpinski, arXiv:0911.0338v2, Phys. Rev. B (to be published).
[16] J. T. Park, D. S. Inosov, Ch. Niedermayer, G. L. Sun, D. Haug, N. B. Christensen, R. Dinnebier, A. V. Boris, A. J. Drew, L. Schulz, T. Shapoval, U. Wolff, V. Neu, X. Yang, C. T. Lin, B. Keimer, and V. Hinkov, Phys. Rev. Lett. **102**, 117006 (2009).
[17] Y. Laplace, J. Bobroff, F. Rullier-Albenque, D. Colson, and A. Forget, Phys. Rev. B **80**, 140501(R) (2009).
[18] D. K. Pratt, W. Tian, A. Kreyssig, J. L. Zarestky, S. Nandi, N. Ni, S. L. Bud'ko, P. C. Canfield, A. I. Goldman, and R. J. McQueeney, Phys. Rev. Lett. **103**, 087001 (2009).
[19] N. Ni, M. E. Tillman, J.-Q. Yan, A. Kracher, S. T. Hannahs, S. L. Bud'ko, and P. C. Canfield, Phys. Rev. B **78**, 214515 (2008).
[20] T. Terashima, M. Kimata, H. Satsukawa, A. Harada, K. Hazama, S. Uji, H. S. Suzuki, T. Matsumoto, and K. Murata, J. Phys. Soc. Jpn. **78**, 083701 (2009).
[21] E. Colombier, S. L. Bud'ko, N. Ni, and P. C. Canfield, Phys. Rev. B **79**, 224518 (2009).
[22] S. A. Baily, Y. Kohama, H. Hiramatsu, B. Maiorov, F. F. Balakirev, M. Hirano, and H. Hosono, Phys. Rev. Lett. **102**, 117004 (2009).
[23] E.-M. Choi, S.-G. Jung, N. H. Lee, Y.-S. Kwon, W. N. Kang, D. H. Kim, M.-H. Jung, S.-I. Lee, and L. Sun, Appl. Phys. Lett. **95**, 062507 (2009).
[24] J. S. Kim, S. Khim, L. Yan, N. Manivannan, Y. Liu, I. Kim, G. R. Stewart, and K. H. Kim, J. Phys.: Condens. Matter **21**, 102203 (2009).
[25] M. A. Tanatar, N. Ni, C. Martin, R. T. Gordon, H. Kim, V. G. Kogan, G. D. Samolyuk, S. L. Bud'ko, P. C. Canfield, and R. Prozorov, Phys. Rev. B **79**, 094507 (2009).
[26] Y. Nakajima, T. Taen, and T. Tamegai, J. Phys. Soc. Jpn. **78**, 023702 (2009).
[27] N. Kumar, R. Nagalakshmi, R. Kulkarni, P. L. Paulose, A. K. Nigam, S. K. Dhar, and A. Thamizhavel, Phys. Rev. B **79**, 012504 (2009).
[28] D. L. Sun, Y. Liu, and C. T. Lin, Phys. Rev. B **80**, 144515 (2009).
[29] N. Kumar, S. Chi, Y. Chen, K. G. Rana, A. K. Nigam, A. Thamizhavel, W. Ratcliff, S. K. Dhar, and J. W. Lynn, Phys. Rev. B **80**, 144524 (2009).
[30] S. R. Saha, N. P. Butch, K. Kirshenbaum, J. Paglione, and P. Y. Zavalij, Phys. Rev. Lett. **103**, 037005 (2009).
[31] J. S. Kim, T. D. Blasius, E. G. Kim, and G. R. Stewart, J. Phys.: Condens. Matter **21**, 342201 (2009).
[32] F. Ronning, E. D. Bauer, T. Park, S.-H. Baek, H. Sakai, and J. D. Thompson, Phys. Rev. B **79**, 134507 (2009).
[33] E. D. Bauer, F. Ronning, B. L. Scott, and J. D. Thompson, Phys. Rev. B **78**, 172504 (2008).
[34] F. Ronning, N. Kurita, E. D. Bauer, B. L. Scott, T. Park, T. Klimczuk, R. Movshovich, and J. D. Thompson, J. Phys.: Condens. Matter **20**, 342203 (2008).
[35] T. Terashima, M. Kimata, H. Satsukawa, A. Harada, K. Hazama, S. Uji, H. Harima, G.-F. Chen, J.-L. Luo, and N.-L. Wang, J. Phys. Soc. Jpn. **78**, 063702 (2009).
[36] N. Kurita, F. Ronning, Y. Tokiwa, E. D. Bauer, A. Subedi, D. J. Singh, J. D. Thompson, and R. Movshovich, Phys. Rev. Lett. **102**, 147004 (2009).

[37] Y. Tomioka, S. Ishida, M. Nakajima, T. Ito, H. Kito, A. Iyo, H. Eisaki, and S. Uchida, Phys. Rev. B **79**, 132506 (2009).
[38] H. Kotegawa, H. Sugawara, and H. Tou, J. Phys. Soc. Jpn. **78**, 013709 (2009).
[39] M. S. Torikachvili, S. L. Bud'ko, N. Ni, and P. C. Canfield, Phys. Rev. Lett. **101**, 057006 (2008).
[40] M. S. Torikachvili, S. L. Bud'ko, N. Ni, P. C. Canfield, and S. T. Hannahs, Phys. Rev. B **80**, 014521 (2009).
[41] G. F. Chen, Z. Li, J. Dong, G. Li, W. Z. Hu, X. D. Zhang, X. H. Song, P. Zheng, N. L. Wang, and J. L. Luo, Phys. Rev. B **78**, 224512 (2008).
[42] Z. Bukowski, S. Weyeneth, R. Puzniak, P. Moll, S. Katrych, N. D. Zhigadlo, J. Karpinski, H. Keller, and B. Batlogg, Phys. Rev. B **79**, 104521 (2009).
[43] U. Welp, R. Xie, A. E. Koshelev, W. K. Kwok, H. Q. Luo, Z. S. Wang, G. Mu, and H. H. Wen, Phys. Rev. B **79**, 094505 (2009).
[44] H.-J. Kim, Y. Liu, Y. S. Oh, S. Khim, I. Kim, G. R. Stewart, and K. H. Kim, Phys. Rev. B **79**, 014514 (2009).
[45] M. M. Altarawneh, K. Collar, C. H. Mielke, N. Ni, S. L. Bud'ko, and P. C. Canfield, Phys. Rev. B **78**, 220505(R) (2008).
[46] Z.-S. Wang, H.-Q. Luo, C. Ren, and H.-H. Wen, Phys. Rev. B **78**, 140501(R) (2008).
[47] N. Ni, S. L. Bud'ko, A. Kreyssig, S. Nandi, G. E. Rustan, A. I. Goldman, S. Gupta, J. D. Corbett, A. Kracher, and P. C. Canfield, Phys. Rev. B **78**, 014507 (2008).
[48] H. Q. Yuan, J. Singleton, F. F. Balakirev, S. A. Baily, G. F. Chen, J. L. Luo, and N. L. Wang, Nature (London) **457**, 565 (2009).
[49] N. R. Werthamer, E. Helfland, and P. C. Hohenberg, Phys. Rev. **147**, 295 (1966).
[50] M. Putti, I. Pallecchi, E. Bellingeri, M. Tropeano, C. Ferdeghini, A. Palenzona, C. Tarantini, A. Yamamoto, J. Jiang, J. Jaroszynski, F. Kametani, D. Abraimov, A. Polyanskii, J. D. Weiss, E. E. Hellstrom, A. Gurevich, D. C. Larbalestier, R. Jin, B. C. Sales, A. S. Sefat, M. A. McGuire, D. Mandrus, P. Cheng, Y. Jia, H. H. Wen, S. Lee, and C. B. Eom, arXiv:0910.1297 (unpublished).
[51] Y. Yin, M. Zech, T. L. Williams, X. F. Wang, G. Wu, X. H. Chen, and J. E. Hoffman, Phys. Rev. Lett. **102**, 097002 (2009).
[52] R. Prozorov, N. Ni, M. A. Tanatar, V. G. Kogan, R. T. Gordon, C. Martin, E. C. Blomberg, P. Prommapan, J. Q. Yan, S. L. Bud'ko, and P. C. Canfield, Phys. Rev. B **78**, 224506 (2008).
[53] A. S. Sefat, R. Jin, M. A. McGuire, B. C. Sales, D. J. Singh, and D. Mandrus, Phys. Rev. Lett. **101**, 117004 (2008).
[54] S. V. Chong, S. Hashimoto, and K. Kadowaki, arXiv:0908.3284 (unpublished).
[55] R. Khasanov, A. Maisuradze, H. Maeter, A. Kwadrin, H. Luetkens, A. Amato, W. Schnelle, H. Rosner, A. Leithe-Jasper, and H.-H. Klauss, Phys. Rev. Lett. **103**, 067010 (2009).
[56] H. Ding, P. Richard, K. Nakayama, K. Sugawara, T. Arakane, Y. Sekiba, A. Takayama, S. Souma, T. Sato, T. Takahashi, Z. Wang, X. Dai, Z. Fang, G. F. Chen, J. L. Luo, and N. L. Wang, EPL **83**, 47001 (2008).
[57] P. L. Alireza, Y. T. C. Ko, J. Gillett, C. M. Petrone, J. M. Cole, G. G. Lonzarich, and S. E. Sebastian, J. Phys.: Condens. Matter **21**, 012208 (2009).
[58] R. T. Gordon, C. Martin, H. Kim, N. Ni, M. A. Tanatar, J. Schmalian, I. I. Mazin, S. L. Bud'ko, P. C. Canfield, and R. Prozorov, Phys. Rev. B **79**, 100506(R) (2009).